Chapter 7

Kinetic Study of the Partial Hydrogenation of 1-Heptyne over Ni and Pd Supported on Alumina

M. Juliana Maccarrone, Gerardo C. Torres, Cecilia Lederhos, Carolina Betti, Juan M. Badano, Mónica Quiroga and Juan Yori

Additional information is available at the end of the chapter

http://dx.doi.org/10.5772/48699

1. Introduction

Selective hydrogenation reactions are industrially used for the partial hydrogenation of unsaturated organic compounds in order to form more stable products or intermediate materials for different processes. The production of final organic products of high added value or intermediate compounds for the synthesis of fine chemicals is both of industrial and academic importance [1]. Alkenes are much appreciated products used in the food industry (flavours), the pharmaceutical industry (sedatives, anesthetises, vitamins) and in the perfumes industry (fragrances). They are also used for the production of biologically active compounds [2], resins, polymers and lubricants, etc.

The partial hydrogenation of acetylenic compounds using homogeneous or heterogeneous metallic catalysts provides a very viable and economically feasible way for the obtaining of these olefinic compounds. Selective catalysts and optimum operational conditions are necessary in order to avoid the complete hydrogenation of the unsaturated bond. Certain transition metals anchored on different solids have demonstrated to be very active and selective catalysts for this type of reaction. They also have the advantage that they can be operated under milder reaction conditions. It is well documented that palladium is a highly active catalyst for hydrogenation [3]. In this sense, Lindlar catalyst ($Pd/CaCO_3$, 5 wt % of Pd modified with $Pb(OAc)_2$) has been used since 1952 as an excellent commercial catalyst for this type of reactions [4]. The argued reasons for the differences in reactivity of Pd indicate that when the metal is electron deficient it becomes less active because alkynes are more weakly adsorbed [5].

During decades a lot of research has been carried out modifying this type of catalysts in order to increase the activity and selectivity: different supports as alumina, coal, silica [5-7] have been tried while modified palladium [8], or nanoparticles of Pd have also been

investigated [9-11]. In a recent work of our group very high activities and selectivities of W monometallic and W-Pd bimetallic catalysts were found during the partial hydrogenation of a long chain terminal alkyne [12]. In this contribution it was reported that important variations in the activity and selectivity were produced when the employed pretreatment conditions were changed. The published reports do not give a clear explanation of the effect of each metal.

Providing an economic, active and selective metallic catalyst for the production of alkenes via selective hydrogenation is a very important challenge. Besides the bibliography on the kinetics of the reaction of heavy alkynes is scarce [13-15]. In this sense, the kinetic study of the liquid phase hydrogenation reaction of 1-heptyne using monometallic nickel and palladium catalysts anchored on γ-alumina made in the current work had three principal objectives: i) to gain knowledge about the reaction system, ii) to obtain kinetic expressions which enable the design of partial hydrogenation reactors, and iii) to give an explanation of the catalytic effect of different metals. The kinetic modelling was used in this work to shed light on these issues.

2. Experimental

2.1. Catalyst preparation

The catalysts were prepared by the incipient wetness technique using Ketjen CK300 γ-Al_2O_3 as support (cylinders of 1.5 mm, calcined at 823K during 4 h, 180 $m^2\ g^{-1}$ BET surface area). To study the influence of metals, acidic solutions with pH=1 were prepared using $NiCl_2$ (Merk Cat. No. 806722), and $Pd(NO_3)_2$ (Fluka, Cat. No. 76070) to prepare the monometallic catalysts. The concentration of the solutions was adjusted in order to obtain metal loading of 4 and 0.4 wt % of Ni and Pd, respectively. The impregnated solids were dried during 24 h at 373 K and then they were calcined in an air flow at 823 K during 3 h. Prior to reaction, the catalysts were reduced in hydrogen flow (105 mL min^{-1}) during 1 h at 673 K for Ni/Al_2O_3 and at 573 K for Pd/Al_2O_3.

2.2. Characterization

2.2.1. Chemical analysis

The metal loadings of the catalysts were determined by digesting the samples and then analyzing the liquors by inductively coupled plasma analysis (ICP) in an OPTIMA 2100 DV Perkin Elmer equipment.

2.2.2. X-Ray Photoelectron Spectroscopy (XPS)

XPS determinations were made in Multitech UniSpecs XR-50 equipment with a dual Mg/Al X-ray source. A SPECS PHOIBOS 150 hemisphere analyzer was used in the Fixed Analyzer Transmission mode (FAT). The samples were treated *ex situ* with a hydrogen flow during 1 h at the corresponding reduction temperature and *in situ* in the load camera of the

instrument with a H_2/Ar (5% v/v) flow during 10 min. The spectra were obtained using pass energy of 30 eV and a Mg anode operated at 200 W. During the tests the pressure was less than 2 10^{-12} MPa.

2.2.3. X-Ray Diffraction (XRD)

X-Ray Diffraction (XRD) measurements of the samples were obtained using a Shimadzu XD-D1 instrument with CuKα radiation (λ = 1.5405A°) in the 15 < 2θ < 85° at a scan speed of 1° min^{-1}. Samples were powdered and reduced under a hydrogen flow, then they were immediately put into the chamber of the equipment and the data acquisition was started.

2.2.4. Temperature Programmed Reduction (TPR)

The tests were performed in an Ohkura 2002 S apparatus equipped with a thermal conductivity detector. A cold water trap was placed before the thermal detector to condense water. Before the TPR tests the samples were dried *in situ* at 673 K for 30 min in an oxygen flow (AGA purity 99.99%). After that the samples were cooled down up to 298 K in an argon flow. Then the temperature was increased up to 1223 K at 10 K min^{-1} in a H_2/Ar (5% v/v) gas flow.

2.2.5. Hydrogen chemisorption

Hydrogen chemisorption was performed by means of the dynamic pulse method using a Micromeritics Auto Chem II apparatus equipped with a thermal conductivity detector. 0.2 g of the samples were reduced 1 h *in situ* at the above mentioned temperatures using a H_2/Ar (5% v/v) flow. The samples were degassed *in situ* for 2 h under an argon flow (AGA, 99.99%) at a temperature equal to that of the corresponding reduction step and then cooled down to room temperature. In the case of the palladium catalysts they were cooled down to 373 K to make the formation of palladium hydride negligible [16]. After that the chemisorption of hydrogen was performed until total saturation of the samples.

2.3. Catalytic tests

The partial hydrogenation of 1-heptyne was carried out in a stainless steel stirred batch reactor equipped with a magnetically coupled stirrer with two blades in counter-rotation that was operated at 800 rpm. The inner wall of the reactor was completely coated with PTFE lining in order to prevent the catalytic action of steel reported by other authors [17]. The tests were performed using the following conditions: partial pressure of H_2 equal to 1.4, 1.9, 2.4 bar; reaction temperature: 293, 303, 323 K; initial 1-heptyne concentration of 0.1019, 0.1528, 0.2038 mol L^{-1}; particle size: fractions of 60 or 120 mesh and 1500 μm. 1-heptyne (Fluka, Cat. No. 51950, >98%), the reactant, was dissolved in toluene (Merck, Cat. No. TX0735-44, >99%). 75 mL of the stock solution and catalyst samples of 0.3 g of Ni/Al_2O_3 and 0.03 g of Pd/Al_2O_3 previously reduced in hydrogen for 1 h at 673 and 573K, respectively, were used in the different catalytic tests.

The evolutions of reactant and products concentrations with reaction time were followed by Gas Chromatography using a flame ionization detector (FID) and a capillary column 30 m J&W INNOWax 19091N-213.

3. Results and discussion

3.1. Catalysts characterization

The metal loadings of the catalysts determined by ICP were 3.5 and 0.35 wt % of Ni and Pd, respectively.

For the monometallic Ni/Al_2O_3 catalyst no hydrogen consumption was detected during the chemisorption analysis, in total accordance with previously reported results [18]. For the Pd/Al_2O_3 catalyst a chemisorption value of 18 μmol H_2 g_{cat}^{-1} was measured.

Figures 1 and 2 show the XPS spectra of Ni $2p_{3/2}$ and Pd 3d for Ni/Al_2O_3 and Pd/Al_2O_3 catalysts, respectively. It can be seen that the monometallic nickel catalyst presents two

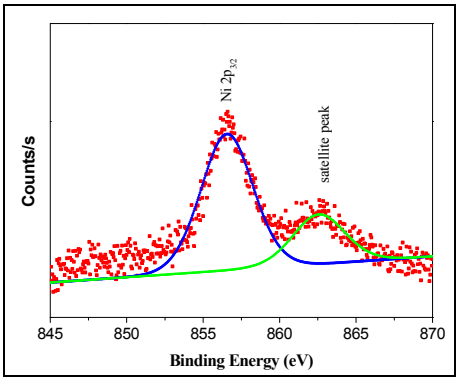

Figure 1. XPS Ni $2p_{3/2}$ spectra of Ni/Al_2O_3.

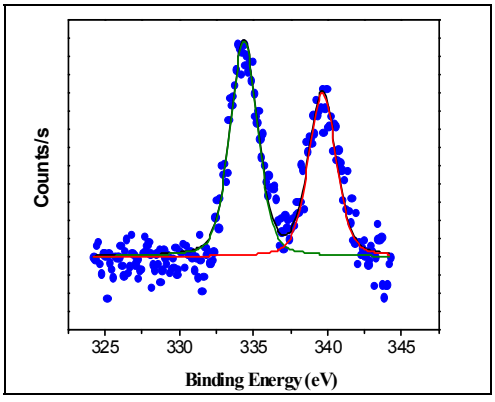

Figure 2. XPS Pd 3d spectra of Pd/Al_2O_3

peaks, with maximums at 855.4 eV and 862.6 eV. The former can be associated to Ni^{2+} species [19-22]; the other peak corresponds to the shake up of Ni(II) [25,28,29]. According to the literature, the maximum BE of the Pd $3d_{5/2}$ peak of the monometallic palladium catalyst at 334.9 eV, with its $3d_{3/2}$ doublet peak at 340.1 eV, corresponds to Pd^0 [18-19,22-23].

The XRD difractograms of the catalysts only present the γ-alumina peaks at 2θ = 37.7, 46.0 and 67.0º [24-26]. For this reason the difractograms are not shown. Because of the low amount of Pd or Ni on the Pd/Al_2O_3 or Ni/Al_2O_3 catalysts, the crystalline phases of palladium or nickel were undetectable. Several authors stated that high charges of nickel (>>15 wt %) are necessary to observe the peaks at 2θ = 43.3°; 63.0°; 75.5° and 79.5° of NiO [27,28].

Figure 3 shows the TPR traces of the studied catalysts. The TPR trace of the Pd monometallic catalyst had a main hydrogen consumption peak at 287 K, which can be attributed to the reduction of PdO species and to the formation of palladium hydrides [29]. This catalyst also has an inverted reduction peak at 339 K that could be related to the decomposition of the β-PdH phase [20,21,24]. As these species interact weakly with the support the palladium hydrides are completely eliminated during reduction. Figure 3 also shows the profile of reduction of Ni/Al_2O_3 catalyst, the principal reduction peak begins at 700 K, finishes over 900 K and presents a maximum at 802 K which corresponds to the reduction of NiO (Ni^{2+} species) interacting with the alumina [30]. The second peak of minor intensity is observed at higher temperatures (>1000 K), and corresponds to the reduction of nickel aluminates [31-32]. At the reduction temperature used during the preparation of the catalysts, the obtained TPR spectra suggest the presence of species Ni^{2+} and Pd^0 on Ni/Al_2O_3 and Pd/Al_2O_3 catalysts, respectively. These results are in total agreement with the XPS results.

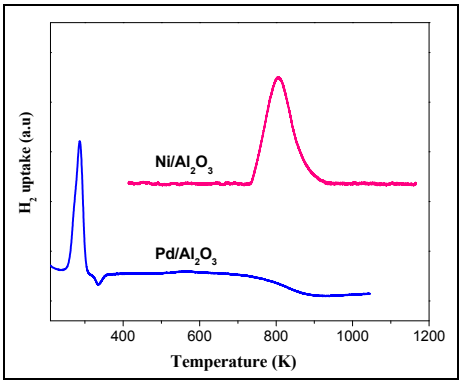

Figure 3. TPR traces of the Ni/Al_2O_3 and Pd/Al_2O_3 catalysts.

It must be noted that the characterization techniques suggest that, after the pretreatment conditions employed during the preparation of the catalysts, only one type of active site is present on each catalytic system.

3.2. Catalytic results

3.2.1. Partial hydrogenation of 1-heptyne

Before considering kinetic expressions or comparing catalyst performances it is necessary to check whether the selected reaction system proceeds in kinetic regime. The possibility of external and internal diffusional limitations during the catalytic tests was thus experimentally assessed.

3.2.1.1. Experimental verification of the absence of external and internal mass transfer limitations

In order to eliminate external diffusional limitations, experiences were carried out using different stirring speeds in the range of 180-1400 rpm. It was found that at stirring rates higher than 500 rpm, 1-heptyne conversion values remained constant, indicating that external gas-liquid limitations were absent. A stirring rate of 800 rpm was therefore chosen for all the kinetic tests. On the other hand and in order to ensure that the catalytic results were not influenced by external and intraparticle mass transfer limitations, the catalyst pellets were milled to samples of different particle size: a fraction bigger than 100 mesh (<150 μm), a fraction of 60-100 mesh (250-150 μm) and pellets of 1500 μm (not milled). The obtained values of 1-heptyne conversion were the same for the two milled fractions indicating the absence of internal diffusional limitations. Then particles with sizes smaller than 250 μm were used in all tests.

3.2.1.2. Catalytic activity results

The catalytic activity results for the partial hydrogenation of 1-heptyne are shown in Figures 4 and 5, where it is represented the variation of 1-heptyne (C_A) and 1-heptene (C_B) concentration as a function of the reaction time for the Ni/Al_2O_3 and Pd/Al_2O_3 catalysts.

It can be clearly seen that Pd is more active than Ni, even when using one tenth of the catalyst mass of the Ni catalyst. Reasons for the differences in reactivity can be found in the literature. Most authors report that when the metal is more electron deficient it becomes less active because alkynes are more weakly adsorbed [5,33]. Nothing however is commented about the role of hydrogen. The published reports do not give a clear explanation of the effect of each metal and for this reason kinetic modelling was used in this work to shed light on these issues.

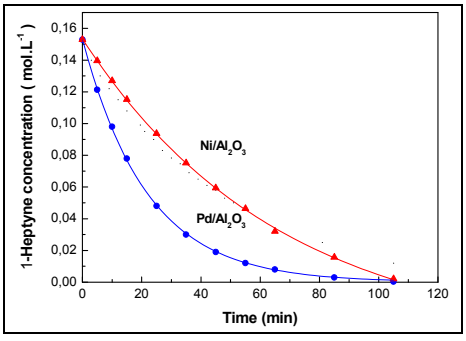

Figure 4. C_A vs. reaction time. P_{H2} =1.4 bar, C^0_A= 0.1528 mol L^{-1}, T= 323 K, 800 rpm, W_{cat}= 0.3 $g_{Ni/Al2O3}$ or 0.03 g $_{Pd/Al2O3}$, S/Ni = 64 and S/Pd = 29385.

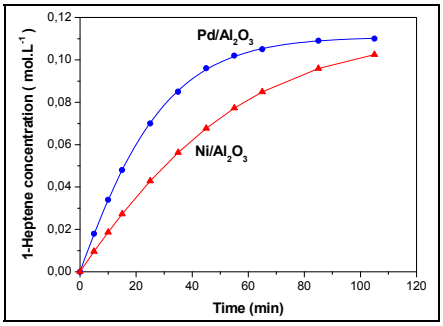

Figure 5. C_B vs. reaction time. P_{H2} =1.4 bar, C_{0A}= 0.1528 mol L^{-1}, T= 323 K, 800 rpm, W_{cat}= 0.3 $g_{Ni/Al2O3}$ or 0.03 g $_{Pd/Al2O3}$, S/Ni = 64 and S/Pd = 29385.

4. Kinetic modeling

4.1. Reaction network

A series-parallel reaction network was proposed for partial hydrogenation of 1-heptyne [14], as indicated in Figure 6.a. This is composed of three hydrogenation reactions that can be a priori considered reversible. The equilibrium constant for each of the previous reactions were calculated using Joback's group contribution method [34]. The values at 323 K were calculated as K_1=3.35 10^{21}, K_2=1.87 10^{35} and K_3=5.58 10^{13}. These values indicate that the individual reactions in Figure 6.a can be considered as irreversible. The experimentally obtained values of total conversion of 1-heptyne confirmed this prediction.

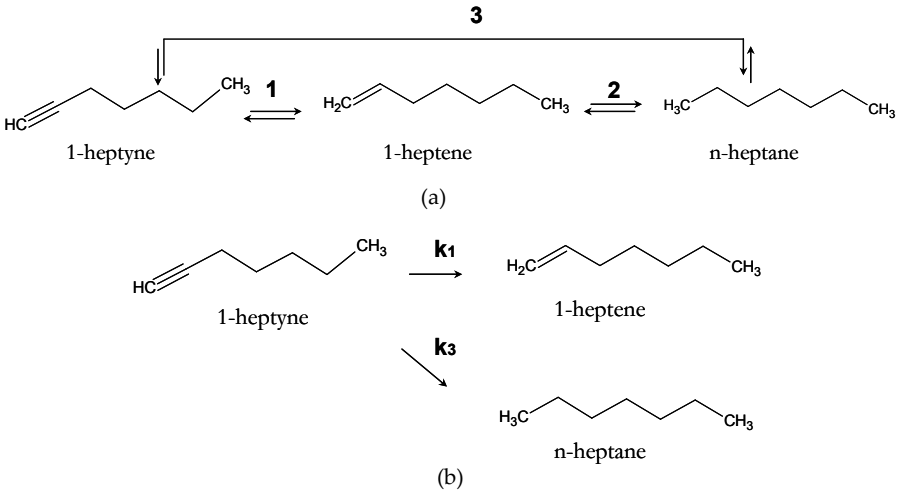

Figure 6. Reaction scheme for 1-heptyne (a) reversible hydrogenation and (b) irreversible hydrogenation.

Experimentally, it is observed that while 1-heptyne is present in the reaction medium, 1-heptene concentration always increases, showing higher concentration than n-heptane.

After all 1-heptyne was consumed, 1-heptene concentration begins to decrease very slowly and n-heptane concentration equally increases. These profiles are consistent with two reaction schemes: i) two parallel irreversible reactions (steps 1 and 3), and ii) series-parallel irreversible reactions, with a k_1/k_2 value higher than 100. The latter considerations, allows us to disregard step 2. Therefore a simplified network of parallel reactions for 1-heptyne hydrogenation can be assumed in Figure 6.b.

4.2. Langmuir-Hinshelwood-Hougen-Watson (LHHW) models

Models of heterogeneous reactions were outlined using the Langmuir-Hinshelwood-Hougen-Watson formalism (LHHW models). Taking into account the previously presented characterization results of Ni/Al_2O_3 and Pd/Al_2O_3, in all the models only one type of active sites was considered to be present. Six different models with their respective basic hypotheses are presented in Table 1. The elementary steps with H_2 dissociative or non-dissociative adsorption reaction mechanism are presented in Table 2.

Mo-del	Hypothesis of the model	Simplified Rate	Parameters
I	Controlling step: adsorption of H_2. Dissociative adsorption of H_2 [42]. Competitive adsorption of 1-heptyne and H_2. Total coverage of active sites.	$r = \frac{P_3}{\left[C_A + P_1.C_B + P_2.C_C\right]^2}$	$P_1 = \frac{K_B}{K_A} \quad P_2 = \frac{K_C}{K_A}$ $P_3 = \frac{k_{H_2}.C_{H_2}.C_S^2}{K_A^2}$
II	Controlling step: adsorption of 1-Heptyne. Dissociative adsorption of H_2 [42]. Competitive adsorption of 1-heptyne and H_2. Total coverage of active sites.	$r = \frac{P_6.C_A}{\left[1 + P_4.C_B + P_5.C_C\right]}$	$P_4 = \frac{K_B}{\sqrt{K_{H_2}.C_{H_2}}}$ $P_5 = \frac{K_C}{\sqrt{K_{H_2}.C_{H_2}}}$ ..
III	Controlling step: surface chemical reaction. Dissociative adsorption of H_2 [42]. Competitive adsorption of 1-heptyne and H_2. Total coverage of active sites.	$r_1 = \frac{P_{10}.C_A}{\left[1 + P_7.C_A + P_4.C_B + P_5.C_C\right]^3}$ $r_3 = \frac{P_{11}.C_A}{\left[1 + P_7.C_A + P_4.C_B + P_5.C_C\right]^3}$	$P_6 = \frac{k_A.C_S}{\sqrt{K_{H_2}.C_{H_2}}}$ $P_7 = \frac{\left(1 + K.K_{H_2}.C_{H_2}\right).K_A}{\sqrt{K_{H_2}.C_{H_2}}}$ $P_{10} = \frac{k_1.K_A.C_S^3}{\sqrt{K_{H_2}.C_{H_2}}}$ $P_{11} = \frac{k_3.K_A.K.C_S^3}{\sqrt{K_{H_2}.C_{H_2}}}$
IV	Controlling step: adsorption of H_2. Non dissociative adsorption of H_2 [43]. Competitive adsorption of 1-heptyne and H_2. The active sites are not completely covered.	$r = \frac{P_{12}}{\left[1 + K_A.C_A + K_B.C_B + K_C.C_C\right]}$	$P_{12} = k'_{H_2}.C_{H_2}.C_S$

Model	Hypothesis of the model	Simplified Rate	Parameters
V	Controlling step: adsorption of 1-Heptyne. Non dissociative adsorption of H_2 [43]. Competitive adsorption of 1-heptyne and H_2. The active sites are not completely covered.	$r = \frac{P_{14}.C_A}{\left[1 + P_{13} + K_B.C_B + K_C.C_C\right]}$	$P_{13} = K^*_{H_2}.C_{H_2}$ $P_{14} = k_A.C_S$
VI	Controlling step: surface chemical reaction. Non dissociative adsorption of H_2 [43]. Competitive adsorption of 1-heptyne and H_2. The active sites are not completely covered.	$r_1 = \frac{P_{16}.C_A}{\left[1 + P_{13} + P_{15}.C_A + K_B.C_B + K_C.C_C\right]^2}$ $r_3 = \frac{P_{17}.C_A}{\left[1 + P_{13} + P_{15}.C_A + K_B.C_B + K_C.C_C\right]^2}$	$P_{15} = \left(1 + K^*.K^*_{H_2}.C_{H_2}\right).K_A$ $P_{16} = k_1.K_A.K^*_{H_2}.C_{H_2}.C_S^2$ $P_{17} = k_3.K_A.K^*.K^{*2}_{H_2}.C^2_{H_2}.C_S^2$

Table 1. LHHW kinetic models.

H_2 dissociative adsorption.		H_2 non dissociative adsorption.	
$H_2 + 2S \Leftrightarrow 2\,HS \quad K_{H_2} = \frac{C^2_{HS}}{C_{H_2}.C^2_S}$	(1)	$H_2 + S \Leftrightarrow H_2S \quad K^*_{H_2} = \frac{C_{H_sS}}{C_{H_2}.C_S}$	(8)
$A + S \Leftrightarrow AS \quad K_A = \frac{C_{AS}}{C_A.C_S}$	(2)	$A + S \Leftrightarrow AS \quad K_A = \frac{C_{AS}}{C_A.C_S}$	(9)
$AS + 2HS \rightarrow BS + 2S \quad K_1 = \infty$	(3)	$AS + H_2S \rightarrow BS + S \quad K_1 = \infty$	(10)
$AS + 2HS \Leftrightarrow AH_2S + 2S \quad K = \frac{C_{AH_2S}.C^2_S}{C_{AS}.C^2_{HS}}$	(4)	$AS + H_2S \Leftrightarrow AH_2S + S \quad K^* = \frac{C_{AH_2S}.C_S}{C_{AS}.C_{H_2S}}$	(11)
$AH_2S + 2\,HS \rightarrow CS + 2S \quad K_3 = \infty$	(5)	$AH_2S + H_2S \rightarrow CS + S \quad K_3 = \infty$	(12)
$BS \Leftrightarrow B + S \quad \frac{1}{K_B} = \frac{C_B.C_S}{C_{BS}}$	(6)	$BS \Leftrightarrow B + S \quad \frac{1}{K_B} = \frac{C_B.C_S}{C_{BS}}$	(13)
$CS \Leftrightarrow C + S \quad \frac{1}{K_C} = \frac{C_C.C_S}{C_{CS}}$	(7)	$CS \Leftrightarrow C + S \quad \frac{1}{K_C} = \frac{C_C.C_S}{C_{CS}}$	(14)

Table 2. Elementary steps with H_2 dissociative or non-dissociative adsorption reaction mechanism.

4.3. Mass balances

The following mass balances for components in the liquid phase were considered for the reaction scheme of Figure 6.b, for 1-heptyne (A), 1-heptene (B) and n-heptane (C):

$$dC_A / dt = -r_1 - r_3 \tag{15}$$

$$dC_B / dt = r_1 \tag{16}$$

$$dC_C / dt = r_3 \quad (17)$$

initial conditions were: t = 0 min, C^0_A = 0.1528 mol L^{-1}, $C^0_B = C^0_C$ = 0 mol L^{-1}.

4.4. Numerical resolution and statistics

The system of differential equations (15)-(17) was solved numerically using the Runge-Kutta-Merson algorithm. The model parameter estimation was performed by a non-linear regression, using a Levenberg-Marquardt algorithm which minimized the objective function:

$$SCD = \sum_j^n \left(C_{i,j} - C_{i,j}^{CALC} \right)^2 \quad (18)$$

where $C_{i,j}$ and $C_{i,j}^{CALC}$ are the experimental and the predicted concentration values, respectively, *"i"* is the chemical compound and *"j"* is the reaction time.

The model adequacy and the discrimination between models were determined using the model selection criterion (MSC), according to the following equation:

$$MSC = ln\left(\frac{\sum_j^n \left(C_{i,j} - \overline{C}_i \right)^2}{\sum_j^n \left(C_{i,j} - C_{i,j}^{CALC} \right)^2} \right) - \left(\frac{2p}{n} \right) \quad (19)$$

where $\overline{C}_i$ is the average relative concentration; p is the amount of parameters fitted and n is the number of experimental data. In order to compare different models, the selected one is that leading to the highest MSC value.

The Standard Deviation (S) was calculated with the following equation:

$$S = \sqrt{s^2} = \sqrt{\frac{\sum_j^n \left(C_{i,j} - C_{i,j}^{CALC} \right)^2}{n - p}} \quad (20)$$

4.5. Model discrimination

The first main requisite for appropriateness of a model should be that of physical significance. A priori this means that the model parameters adopt feasible real values. A second requisite is that of adequate statistical confidence, i.e. the parameters should lie in one as small as possible confidence interval.

The practical criteria for the selection of the kinetic models were:

1. The estimated values of the parameters must be positive and different from zero.
2. The upper and lower extremes of the confidence interval (95%) must be positive.

3. The amplitude of the confidence interval must be lower than the value of the estimated parameter.

The final model is selected from the set of models complying the above 1 to 3 conditions, as the model with the lowest SCD, the summation of squares of the deviations. Another condition is that the standard deviation is smaller than the value of the parameter. If differences are not big, then the model selection criterion (MSC) should be used. Appropriate models should have a MSC value greater than 4.

4.6. Kinetic models for the reaction

Preliminary tests were performed in order to check the influence of the different variables on the reaction rate. These results will be used later in the model selection stage. The variables screened were the partial pressure of hydrogen, the initial concentration of 1-heptyne and the reaction temperature. In order to analyze the influence of each variable a pseudo homogeneous reaction model was proposed in which the reaction rate was assumed to follow a potential law. The initial reaction rate should thus be written as:

$$r_A^0 = k.(C_A^0)^{\alpha}.(P_{H2})^{\beta} \tag{21}$$

An Arrhenius dependent was supposed for the specific constant of reaction:

$$k = A.e^{\frac{-E_A}{R.T}} \tag{22}$$

4.6.1. Influence of the partial pressure of hydrogen

Several tests were performed at varying hydrogen partial pressures (1.4, 1.9 and 2.4 bar) keeping all other variables constant (C^0_A= 0.1528 mol L^{-1}, T= 303 K, 800 rpm, W_{cat}= 0.3 g Ni/Al_2O_3 or 0.03 Pd/Al_2O_3). The partial pressure of hydrogen was calculated as the difference between the total pressure and the partial pressure of the solvent, since the partial pressures of 1-heptyne and the products was negligible. The pressure of the solvent at 303 K was determined using Antoine's equation (0.048 bar).

Experimental values of conversion of 1-heptyne as a function of time are plotted in Figures 7.a and 7.b. Both Figures show that as P_{H2} rises, 1-heptyne total conversion increases for Ni/Al_2O_3 catalyst, but decrease for Pd/Al_2O_3. The reaction order with respect to hydrogen (β) was calculated from the linearized form of equation (21).

$$ln(r_A^0) = ln\left[k.\left(C_A^0\right)^{\alpha}\right] + \beta.ln(P_{H2}) \tag{23}$$

The initial reaction rates of 1-heptyne were calculated by polynomial differentiation of the traces of Figures 7.a and 7.b and extrapolation to zero reaction time. From the plot of $ln(r^0_A)$ vs. $ln(P_{H2})$, shown in Figures 8.a and 8.b, reaction order in hydrogen of 1.3 and -2.6 were calculated for Ni/Al_2O_3 and for Pd/Al_2O_3, respectively. The results indicate that: a) for

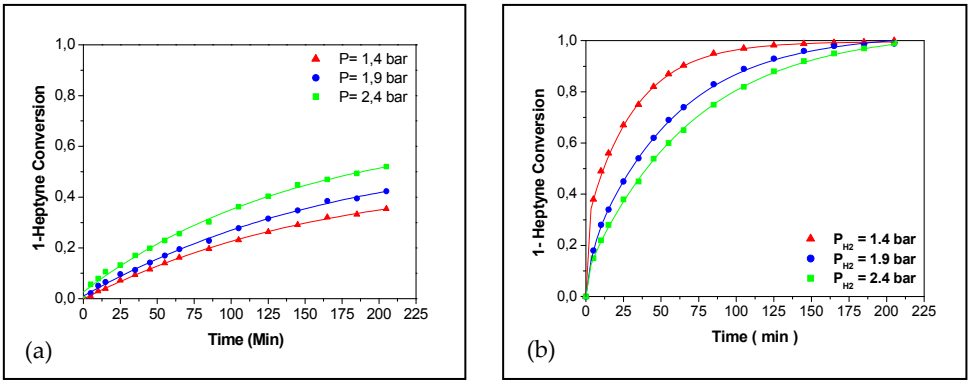

Figure 7. Effect of P_{H2} on the catalytic activity for (a) Ni/Al_2O_3 and (b) Pd/Al_2O_3. C^0_A= 0.1528 mol L^{-1}, T=303 K, 800 rpm, W_{cat}= 0.3 $g_{Ni/Al2O3}$ or 0.03 g $_{Pd/Al2O3}$, S/Ni = 64 and S/Pd =29385.

Ni/Al_2O_3 catalyst, high hydrogen partial pressures are beneficial for the reaction kinetics, probably both adsorption and surface reaction elementary steps could be enhanced; and b) an increase in the partial pressure of hydrogen negatively affects the reaction rate for Pd/Al_2O_3.

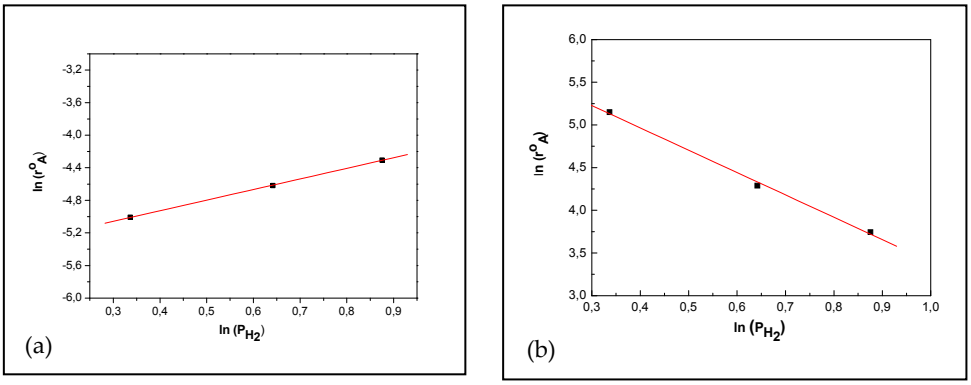

Figure 8. Initial reaction rate as a function of hydrogen pressure for (a) Ni/Al_2O_3 and (b) Pd/Al_2O_3. C^0_A=0.1528 mol L^{-1}, T=303 K, 800 rpm, W_{cat}= 0.3 $g_{Ni/Al2O3}$ or 0.03 g $_{Pd/Al2O3}$, S/Ni = 64 and S/Pd =29385.

4.6.2. Influence of the initial concentration of 1-heptyne

Catalytic tests were performed varying the initial concentration of 1-heptyne: 0.1019, 0.1528 and 0.2038 mol L^{-1}, keeping all the rest of the variables constant (P_{H2}=1.4 bar, T= 303 K, 800 rpm, W_{cat} = 0.3 g Ni/Al_2O_3 or 0.03 Pd/Al_2O_3).

The obtained values of conversion of 1-heptyne as a function of time are plotted in Figures 9.a and 9.b. It can be seen that for both catalysts the catalytic activity is decreased when the initial concentration of 1-heptyne is increased.

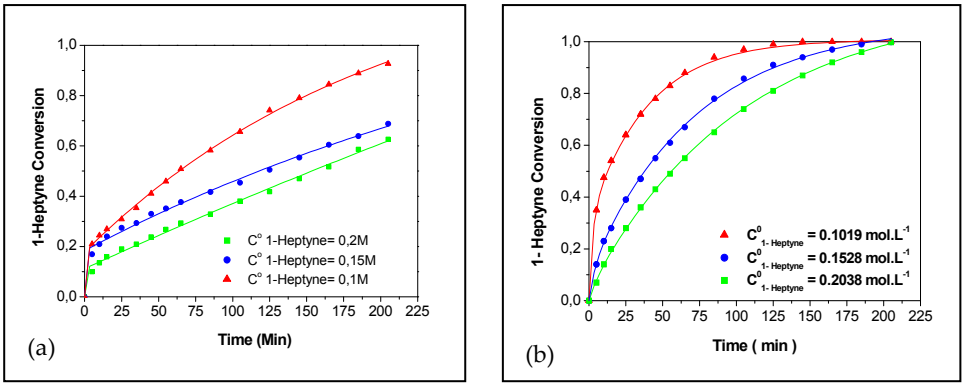

Figure 9. Effect of C^0_A on the catalytic activity for (a) Ni/Al_2O_3 and (b) Pd/Al_2O_3. P_{H2}=1.4 bar, T=303 K, 800 rpm, W_{cat}= 0.3 $g_{Ni/Al2O3}$ or 0.03 g $_{Pd/Al2O3}$, S/Ni = 42, 64 and 85, S/Pd =19596, 29335 and 39192.

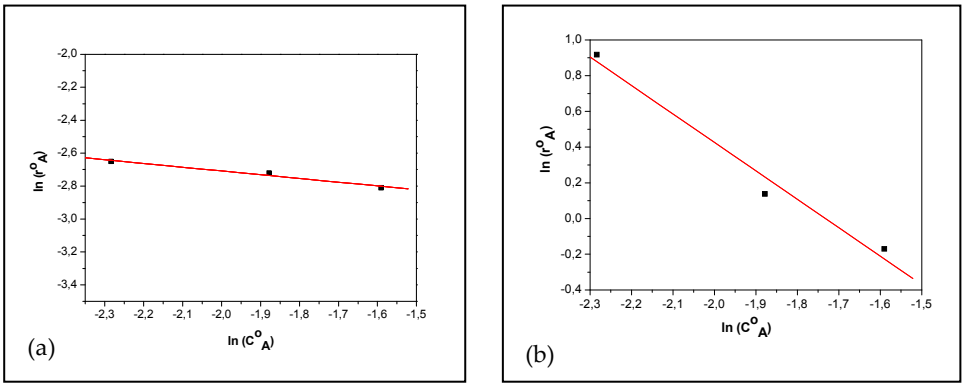

Figure 10. Initial reaction rate of 1-heptyne concentration for (a) Ni/Al_2O_3 and (b) Pd/Al_2O_3. P_{H2}=1.4 bar, T=303 K, 800 rpm, W_{cat}= 0.3 $g_{Ni/Al2O3}$ or 0.03 g $_{Pd/Al2O3}$, S/Ni = 42, 64 and 85, S/Pd =19596, 29335 and 39192.

The value of the reaction order in 1-heptyne (α) can be calculated along the lines described in the previous section:

$$ln(r_A^0) = ln\left[k.\left(P_{H2}\right)^{\beta}\right] + \alpha.ln(C_A^0) \tag{24}$$

The graph of $ln(r^0_A)$ vs. $ln(C^0_A)$, Figures 10.a and 10.b, yields value of order of reaction of 1-heptyne equal to -0.22 and -1.5 for Ni/Al_2O_3 and Pd/Al_2O_3, respectively. The results indicate that an increase in the initial concentration of 1-heptyne is detrimental to the reaction rates.

4.6.3. Influence of the reaction temperature

Catalytic tests were performed varying the reaction temperature: 293, 303 and 323 K, and keeping the rest of the variables constant (P_{H2}=1.4 bar, C^0_A = 0.1528 mol L^{-1}, 800 rpm, W_{cat} = 0.3 g Ni/Al_2O_3 or 0.03 Pd/Al_2O_3).

The experimental values of conversion of 1-heptyne as a function of time at different temperature values are plotted in Figures 11.a and 11.b. As expected the activity of the catalyst is increased while the reaction temperature is raised up.

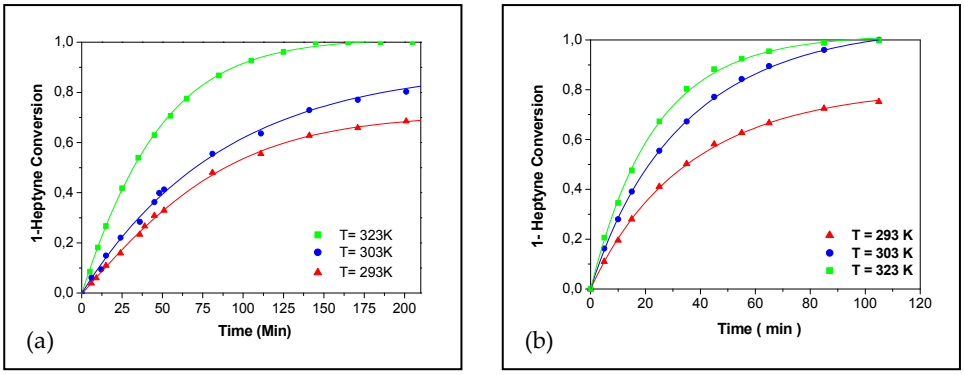

Figure 11. Effect of T on the catalytic activity for (a) Ni/Al_2O_3 and (b) Pd/Al_2O_3. P_{H2}=1.4 bar, 800 rpm, W_{cat}= 0.3 $g_{Ni/Al2O3}$ or 0.03 g $_{Pd/Al2O3}$, S/Ni = 64 and S/Pd = 29385.

When equation (21) is linearized a value of "apparent" activation energy (E_A) can be got, as indicated in Eq. (25):

$$ln(r_A^0) = ln\left[A.(P_{H2})^{\beta}.(C_A^0)^{\alpha}\right] - \frac{E_A}{R.T} \tag{25}$$

The initial reaction rates of 1-heptyne were calculated as in the previous sections. The value of the apparent activation energy were obtained from the plots presented in Figure 12 of $ln(r^0_A)$ as a function of 1/T. The calculated values were 24 and 18 KJ mol^{-1} for Ni/Al_2O_3 and Pd/Al_2O_3, respectively. These values have not a real physical meaning and are only apparent.

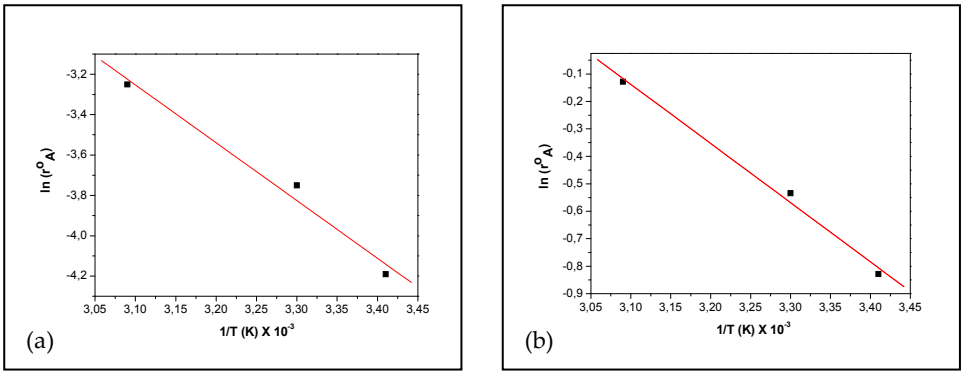

Figure 12. Temperature dependence of the reaction rate for (a) Ni/Al_2O_3 and (b) Pd/Al_2O_3. P_{H2}=1.4 bar, T=303 K, 800 rpm, W_{cat}= 0.3 $g_{Ni/Al2O3}$ or 0.03 g $_{Pd/Al2O3}$, S/Ni = 64 and S/Pd = 29385.

4.6.4. Model discrimination for Ni/Al_2O_3 catalyst

Models II, III, V and VI of Table 1 were discarded because they could not explain the negative and positive orders in 1-heptyne and hydrogen obtained experimentally. The parameters estimated for the models I and IV are indicated in Table 3. A statistical analysis was performed to discriminate between the different models, by means of the selection criteria described in Section 4.5. The results of this analysis are detailed in Table 3. It can be concluded that the best fit is achieved with model I- B. In this model the value of P_2 is equal to zero, indicating that n-heptane is not adsorbed. The model IV-D also shows a good fit of the experimental data, but a pseudo homogeneous kinetic expression is obtained with different reaction orders than those previously calculated.

Model	Option	Estimated parameter (*)	SCD	MSC	Parameter	Parameter sign	Discrimination	Viability
I	A	P_1 = 4.4823237±168.14985673 P_2 = 3.44577501± 335.92334499 P_3 = 0.0001211222587±0.00003376836	$2.1.10^{-3}$	3.7	P_1 P_2 P_3	(+) (+) (+)	IC < 0, CL > VE IC < 0, CL > VE IC < 0, CL > VE	Not viable
	B	P_2 = 0 P_1 = 5.93108434±0.97784253 P_3 = 0.000113720472±0.000026730661	2.10^{-3}	4.5	P_2=0 P_1 P_3	 (+) (+)	 IC > 0, CL < VE IC > 0, CL < VE	Viable
IV	A	K_A= 8.34221367±355.9610964 K_B= -1097.26187±7313.33134 K_C= 2384.39316±12837.26474 P_{12}= 0.00654481117±0.15591798	$2.47.10^{-4}$	5.17	K_A K_B K_C P_{12}	(+) (-) (+) (+)	IC < 0, CL > VE IC < 0, CL > VE IC < 0, CL > VE IC < 0, CL > VE	Not viable
	B	K_A= -6.36443252±3.54535551 K_B= 0 K_C= -17.1237873±50.0933591 P_{12}= $7.82119826.10^{-5}$±$1.570645.10^{-3}$	$2.47.10^{-4}$	5.23	K_A K_B= 0 K_C P_{12}	(-) (-) (+)	IC < 0, CL > VE IC < 0, CL > VE IC < 0, CL > VE	Not viable
	C	K_A= -5.14858364±0.29479977 K_B= 0 K_C= 0 P_{12}= 0.000613057924±$3.87.10^{-5}$	$2.47.10^{-4}$	5.21	K_A K_B= 0 K_C= 0 P_{12}	(-) (+)	IC < 0, CL > VE IC < 0, CL > VE	Not viable
	D	K_A= 0 K_B= 0 K_C= 0 $P_{12}\neq 0$ A pseudohomogeneous model is obtained.			K_A= 0 K_B= 0 K_C= 0 $P_{12}\neq 0$			Viable

Reaction conditions: P_{H2}=1.4 bar, T=323 K, w_{cat}=0.3 g, stirring rate=800 rpm, C^0_A=0.1528 mol.L^{-1}, S/Ni = 64.
(*) 95% confidence interval. IC: confidence interval; CL: confidence level; VE: estimated parameter value

Table 3. Estimated parameters and model discrimination for Ni/Al_2O_3.

Figure 13 contains experimental values of the concentration of 1-heptyne, 1-heptene and n-heptane along with theoretical values (solid line) estimated with model I-B, as a function of

time. A good fit between the two sets of values can be seen. The same regression with model I-B was done with experimental data obtained at other reaction temperatures in the 293-323 K range. In all cases and as a consequence of the fit, parameters different from zero were obtained for a confidence interval of 95% and with values of the MSC parameter greater than 4.0. The thermodynamic consistency of the P_1 and P_3 parameters was graphically evaluated by plotting $\ln P_1$ and $\ln P_3$ as a function of 1/T. In both cases a straight line was obtained (Figure 14) indicating that the constants have an Arrhenius dependence on temperature.

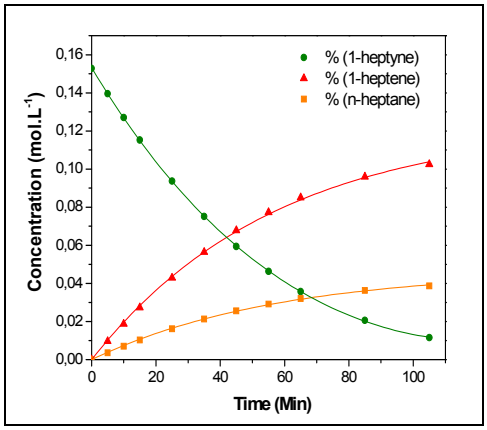

Figure 13. Fit of the experimental data of C_i as a function of time with model I-B for Ni/Al_2O_3 catalyst. P_{H2}=1.4 bar, C^0_A=0.1528 mol L^{-1}, 323 K, W_{cat}=0.3 g, S/Ni = 64.

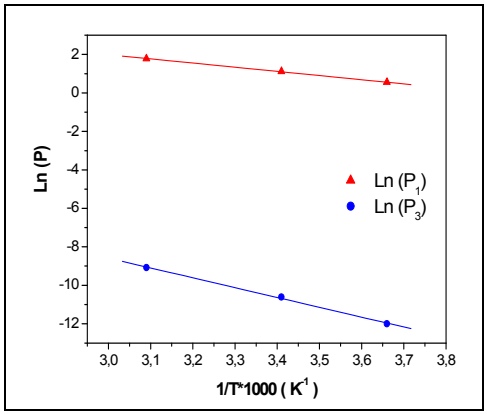

Figure 14. Temperature dependence of parameters P_1 and P_3 for Ni/Al_2O_3 catalyst

The slopes of the straight lines correspond to the values of the enthalpies of adsorption of 1-heptyne and 1-heptene and the value of the energy of activation for the dissociative adsorption of hydrogen on the active sites. Considering the definition of P_1 and P_3, the following equations can be obtained:

$$P_1 = \frac{K_B}{K_A} = \left(\frac{A_B}{A_A}\right).Exp\left[\frac{|\Delta H_B| - |\Delta H_A|}{R.T}\right] \quad (26)$$

$$P_3 = \frac{C_{H2}.k_{H2}.C_S^2}{K_A^2} = \left(\frac{C_{H2}.A_{H2}.C_S^2}{A_A^2}\right).Exp\left[\frac{-(E_{H2} + 2.|\Delta H_A|)}{R.T}\right] \quad (27)$$

In equations (26) and (27) the enthalpies of adsorption of 1-heptyne and 1-heptene were expressed in absolute values. The obtained values from the slopes of the lines in Figure 14 were:

$$|\Delta H_B| - |\Delta H_A| = -17.91 \text{ KJ mol}^{-1} \quad (28)$$

$$E_{H2} + 2.|\Delta H_A| = 58 \text{ KJ mol}^{-1} \quad (29)$$

Considering that $|\Delta H_B| \approx 0$, in accord with the experimental results, a value of the enthalpy of adsorption for 1-heptyne can be obtained from equation (28): ΔH_A = -17.91 KJ mol^{-1}. Introducing this value in equation (29) a value of E_{H2} of 22.2 KJ mol^{-1} can be estimated.

From the results it could be concluded that:

1. Model I-B that supposes dissociative adsorption of hydrogen as the rate-controlling step of reaction and a single type of active sites with total coverage, is the one that best fits experimental data with statistical and thermodynamic consistency.
2. The model does not allow to directly obtain the enthalpies of adsorption of 1-heptyne and 1-heptene and the activation energy for the adsorption of hydrogen.
3. From equation (28) it can be inferred that the enthalpy of adsorption of 1-heptyne is greater than that of 1-heptene, in agreement with the information available in the literature on the partial hydrogenation of alkynes [34].
4. This model also supposes that the alkane is not adsorbed. If we additionally suppose that the enthalpy of adsorption of 1-heptene is negligible, in accordance with experimental results, a value of the enthalpy of adsorption of 1-heptyne and activation energy for the H_2 adsorption can be obtained from eqs. (28) and (29).

Then, it can be concluded that the dissociative adsorption of H_2 is the rate limiting step for the Ni/Al_2O_3 catalyst, and that the active sites are preferentially occupied by 1-heptyne.

4.6.5. Model discrimination for the Pd/Al_2O_3 catalyst

Models I, II, IV and V of Table 1 were discarded because they could not explain the negative orders in 1-heptyne and hydrogen obtained experimentally. The parameters estimated for the models III and VI are indicated in Table 4. A statistical analysis was performed to discriminate between the different models, by means of the selection criteria described in Section 4.5. The results of this analysis are detailed in Table 4; these results indicate that model III-C gives the best fit of the experimental data. In this model the value of the

parameters P_4 and P_5 are equal to zero. Therefore the only species being adsorbed on the Pd/Al_2O_3 catalyst are 1-heptyne and hydrogen.

Model	Option	Estimated parameter (*)	SCD	MSC	Parameter	Parameter sign	Discrimination	Viability
III	A	P_4 = -53.0866055±3399.8626255 P_5 = 221.348971±7134.846189 P_7 = 28.7488806±370.8944874 P_{10} = 4.68720094±147.04798306 P_{11} = 1.92159358±60.33982722	$2.2.10^{-4}$	5.206	P_4 P_5 P_7 P_{10} P_{11}	(-) (+) (+) (+) (+)	IC < 0, CL > VE IC < 0, CL > VE IC < 0, CL > VE IC < 0, CL > VE IC < 0, CL > VE	Not viable
	B	P_4 = 0 P_5 = 73.3086809±919.4831331 P_7 = 23.0235065±284.1617705 P_{10} = 2.75603228±79.34470502 P_{11} = 1.12978185±32.52404635	$2.2.10^{-4}$	5.266	P_5 P_7 P_{10} P_{11}	(+) (+) (+) (+)	IC < 0, CL > VE IC < 0, CL > VE IC < 0, CL > VE IC < 0, CL > VE	Not viable
	C	P_4 = 0 P_5 = 0 P_7 = 0.554228500±0.330992359 P_{10} = 0.0368778035±0.0032648682 P_{11} = 0.0150940473±0.0014453604	$9.1.10^{-5}$	6.23	P_7 P_{10} P_{11}	(+) (+) (+)	IC > 0, CL < VE IC > 0, CL < VE IC > 0, CL < VE	Viable
VI	A	K_B = -16.3714023±661.1021023 K_C = 48.4132846±2509.3986254 P_{13} = 6.35365882±135.97712018 P_{15} = 7.14818320±324.0314528 P_{16} = 2.13263324±47.39641486 P_{17} = 0.874143654±19.422821246	$2.2.10^{-4}$	5.145	K_B K_C P_{13} P_{15} P_{16} P_{17}	(-) (+) (+) (+) (+) (+)	IC < 0, CL > VE IC < 0, CL > VE IC < 0, CL > VE IC < 0, CL > VE IC < 0, CL > VE IC < 0, CL > VE	Not viable
	B	K_B = 0 K_C = 53.7394284±6350.0751416 P_{13} = 3.53653444±247.34456656 P_{15} = 19.8231433±1876.7295967 P_{16} = 1.71129670±50.9810815 P_{17} = 0.702039726±20.910298274	$2.2.10^{-4}$	5.206	K_C P_{13} P_{15} P_{16} P_{17}	(+) (+) (+) (+) (+)	IC < 0, CL > VE IC < 0, CL > VE IC < 0, CL > VE IC < 0, CL > VE IC < 0, CL > VE	Not viable
	C	K_B = 0 K_C = 0 P_{13} = 2.93941739±18.79975681 P_{15} = 1.86782613±10.08702077 P_{16} = 0.541342090±5.18514542 P_{17} = 0.221642448±2.121511182	$2.2.10^{-4}$	5.26	P_{13} P_{15} P_{16} P_{17}	(+) (+) (+) (+)	IC < 0, CL > VE IC < 0, CL > VE IC < 0, CL > VE IC < 0, CL > VE	Not viable
	D	K_B = 0 K_C = 0 P_{13} = 0 P_{15} = 0.610445795±0.825496865 P_{16} = 0.0357150918±0.0052744265 P_{17} = 0.0146412833±0.0023224598	$2.2.10^{-4}$	5.327	P_{15} P_{16} P_{17}	(+) (+) (+)	IC < 0, CL > VE IC > 0, CL < VE IC > 0, CL < VE	Not viable
	E	K_B = 0 K_C = 0 P_{13} = 0 P_{15} = 0 P_{16} = 0.0320548839±0.0012299287 P_{17} = 0.0130965076±0.0007651406	$2.4.10^{-4}$	5.303	P_{16} P_{17}	(+) (+)	IC > 0, CL < VE IC > 0, CL < VE	Viable

Reaction conditions: P_{H2}=1.4 bar, T=323 K, w_{cat}=0.03 g, stirring rate=800 rpm, C^0_A=0.1528 mol.L^{-1}, S/Pd = 29385.
(*) 95% confidence interval. IC: confidence interval; CL: confidence level; VE: estimated parameter value.

Table 4. Estimated model parameters and model discrimination for Pd/Al_2O_3

The heterogeneous model VI-E also produces a good fit of the experimental data but its parameters K_B, K_C, P_{13} and P_{15} are equal to zero, thus transforming into a pseudo homogeneous reaction rate expression in which the reaction orders in 1-heptyne and hydrogen are positive. This is not in agreement with the observed results, so this model was discarded.

Figure 15 contains values of concentration of 1-heptyne, 1-heptene and n-heptane as a function of time, experimentally (symbols) or theoretically obtained (solid line) with the III-C model. There is an excellent fit.

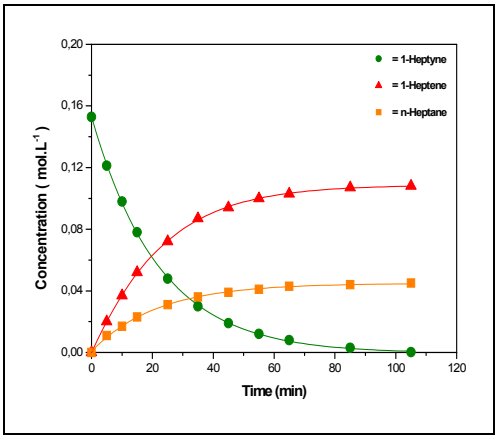

Figure 15. Fit of the experimental data of C_i as a function of time with model III-C for Pd/Al_2O_3 catalyst. P_{H2}=1.4 bar, T=323 K, 800 rpm, W_{cat}= 0.03 g, S/Pd = 29385.

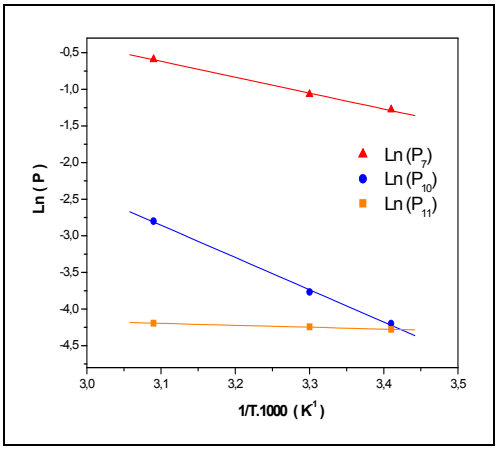

Figure 16. Temperature dependence of parameters P_7, P_{10} and P_{11} for Pd/Al_2O_3 catalyst

The same fit with model III-C was repeated with experimental data at other reaction temperatures in the 293-323 K range. In all cases and as a consequence of the fit, parameters

were obtained with values different from zero in a confidence interval of 95% and with values of the MSC parameter greater than 4.0. The thermodynamic consistence of parameters P_7, P_{10} and P_{11} was evaluated by plotting $\ln P_7$, $\ln P_{10}$ and $\ln P_{11}$ as a function of 1/T. In all cases straight lines were obtained confirming the hypotheses of Arrhenius dependence with respect to temperature (Figure 16).

The slopes of the straight lines obtained correspond to the enthalpies of adsorption of 1-heptyne and H_2 and the energies of activation of the surface reactions of hydrogenation. Taking into account the definition of the parameters P_7, P_{10} and P_{11} (Table 1) the following equations can be obtained:

$$P_7 = \frac{(1 + K.K_{H2}.C_{H2}).K_A}{\sqrt{K_{H2}.C_{H2}}} \tag{30}$$

Supposing that $1 >> K.K_{H2}.C_{H2}$ (this assumption is made for the purpose to estimate some values of the involved constants).

The previous equation is reduced to:

$$P_7 = \frac{K_A}{\sqrt{K_{H2}.C_{H2}}} = \frac{A_A}{\sqrt{A_{H2}.C_{H2}}}.\mathrm{Exp}\left[\frac{-\left(\frac{1}{2}.|\Delta H_{H2}| - |\Delta H_A|\right)}{R.T}\right] \tag{31}$$

$$P_{10} = \frac{k_1.K_A.C_S^3}{\sqrt{K_{H2}.C_{H2}}} = \frac{A_1.A_A.C_S^3}{\sqrt{A_{H2}.C_{H2}}}.\mathrm{Exp}\left[\frac{-\left(E_1 - |\Delta H_A| + \frac{1}{2}.|\Delta H_{H2}|\right)}{R.T}\right] \tag{32}$$

$$P_{11} = \frac{k_3.K_A.K.C_S^3}{\sqrt{K_{H2}.C_{H2}}} = \frac{A_3.A_A.A.C_S^3}{\sqrt{A_{H2}.C_{H2}}}.\mathrm{Exp}\left[\frac{-\left(E_3 - |\Delta H_A| + \Delta H + \frac{1}{2}.|\Delta H_{H2}|\right)}{R.T}\right] \tag{33}$$

In equations (31), (32) and (33) the enthalpies of adsorption of 1-heptyne and H_2 are expressed in absolute values. The values of the respective slopes were calculated as follows:

$$\frac{|\Delta H_{H2}|}{2} - |\Delta H_A| = 18.02 \text{ KJ mol}^{-1} \tag{34}$$

$$E_1 + \frac{|\Delta H_{H2}|}{2} - |\Delta H_A| = 36.6 \text{ KJ mol}^{-1} \tag{35}$$

$$E_3 + \Delta H + \frac{|\Delta H_{H2}|}{2} - |\Delta H_A| = 2.18 \text{ KJ mol}^{-1} \tag{36}$$

The enthalpy of H_2 adsorption on Pd has been reported in Ref. [35] (-75.31 KJ mol^{-1}), then from equation (34): $|\Delta H_A| = 19.64$ KJ mol^{-1}. Replacing eq. (34) into eq. (35): $E_1 = 18.58$ KJ mol^{-1}. From equations (34) and (36):

$$E_3 + \Delta H = -15.84 \text{ KJ mol}^{-1} \quad (37)$$

From the results it can be concluded that:

5. Model III-C that poses the surface chemical reaction as the limiting step is the one that best fits the experimental data. The model also poses the dissociative adsorption of H_2 and the competition with 1-heptyne for the active sites. The model presents statistical and thermodynamic consistency.
6. The model enables obtaining directly the values of the enthalpies of adsorption of 1-heptyne and the activation energy for the hydrogenation of 1-heptyne to 1-heptene (E_1). Neither the calculation of the activation energy for the hydrogenation of 1-heptyne to n-heptane (E_3).
7. The model indicates that 1-heptyne and H_2 are the only species adsorbed on the active sites. The enthalpy of adsorption of 1-heptyne over Pd (-19.64 KJ mol^{-1}) is not much different from the value reported by Semagina et al [36] for the hydrogenation of 1-hexyne over Pd nanoparticles.
8. Equation (34) shows that the enthalpy of adsorption of hydrogen is higher than that of 1-heptyne over the Pd/Al_2O_3 catalyst. This suggests that there are not thermodynamic limitations for the adsorption of H_2. This was confirmed by the tests of hydrogen chemisorptions as Pd is able to chemisorb an important amount of H_2 at room temperature, suggesting that there is not a kinetic impediment as that observed for Ni. Consequently, the dissociative adsorption of hydrogen is fast and then the controlling step is the surface chemical reaction.
9. The value obtained for the activation energy of the hydrogenation reaction of 1-heptyne to 1-heptene (E_1) turned out to be quite low (18.58 KJ mol^{-1}). This coincides with the fact that the reaction can proceed at low temperatures.
10. The kinetic modelling of the reactions over the Ni and Pd catalysts gives an explanation of the different reactivity of the catalysts. Pd is more active than Ni for partial hydrogenation reactions because there is a kinetic limitation for the adsorption of hydrogen on Ni. Hydrogen is more strongly chemisorbed on Pd, so there is a great coverage of the surface by H_2, therefore making the surface reaction step as the rate-controlling one.

5. Conclusions

Pd/Al_2O_3 was more active and selective than Ni/Al_2O_3 for the partial hydrogenation of 1-heptyne to 1-heptene.

In order to analyze the influence of the different variables (hydrogen partial pressure, initial concentration of 1-heptyne and reaction temperature) on the reaction rate a pseudo

homogeneous model was proposed based on power law kinetics. Reaction orders for hydrogen and 1-heptyne were obtained as well as the apparent activation energy. For the Ni/Al_2O_3 catalyst, reaction orders of 1.3 in hydrogen and -0.22 in 1-heptyne, and apparent activation energy of 24 KJ mol^{-1} were obtained. For the Pd/Al_2O_3 catalyst, reaction orders of -2.6 and -1.5 in hydrogen and 1-heptyne, respectively, and apparent activation energy of 18 KJ mol^{-1} were obtained.

In order to elucidate the role of Ni and Pd on the reaction rate, the kinetic data were fitted with six different heterogeneous LHHW models. The results obtained indicate that for the Ni/Al_2O_3 catalyst the controlling step is the dissociative adsorption of hydrogen over the metal active sites and the reaction rate can be expressed by:

$$r = \frac{P_3}{\left[C_A + P_1.C_B\right]^2}$$

If it is assumed that the adsorption enthalpy of 1-heptene can be considered negligible, a value of -17.91 KJ mol^{-1} is obtained for the adsorption enthalpy of 1-heptyne. In the same way, the value of activation energy for the hydrogen adsorption is 22.2 KJ mol^{-1}.

For the Pd/Al_2O_3 catalyst the controlling steps are the surface hydrogenation reactions (1-heptyne to 1-heptene and 1-heptyne to n-heptane). The corresponding reaction rates are:

$$r_1 = \frac{P_{10}.C_A}{\left[1 + P_7.C_A\right]^3} \qquad r_3 = \frac{P_{11}.C_A}{\left[1 + P_7.C_A\right]^3}$$

Using a value for the adsorption enthalpy of hydrogen on Pd reported in literature, a value of -19.64 KJ mol^{-1} is obtained for the adsorption enthalpy of 1-heptyne (ΔH_A) over Pd. Besides, the value obtained for the activation energy for the hydrogenation reaction of 1-heptyne to 1-heptene (E_1) was 18.58 KJ mol^{-1}. This coincides with the fact that the reaction can proceed at low temperatures.

The different activity levels of the Pd/Al_2O_3 and Ni/Al_2O_3 catalysts are due to a kinetic limitation for the adsorption of hydrogen on Ni. In the case of Pd this limitation does not exist.

Author details

M. Juliana Maccarrone, Cecilia Lederhos and Carolina Betti
Institute of Catalysis and Petrochemistry Research, INCAPE (CONICET- UNL), Santa Fe, Argentina

Gerardo C. Torres
Departament of Chemical Engineering Reactions, Faculty of Chemical Engineerin, Santa Fe, Argentina

Juan M. Badano and Mónica Quiroga*
Institute of Catalysis and Petrochemistry Research, INCAPE (CONICET- UNL), Santa Fe, Argentina
Inorganic Chemistry, Departament of Chemistry, Faculty of Chemical Engineering National University of Litoral (UNL), Santa Fe, Argentina

Juan Yori
Institute of Catalysis and Petrochemistry Research, INCAPE (CONICET- UNL), Santa Fe, Argentina
Departament of Chemical Engineering Reactions, Faculty of Chemical Engineering, Santa Fe, Argentina

Acknowledgement

The experimental assistance of C. A. Mázzaro and the financial support provided by UNL and CONICET of Argentina are greatly acknowledged.

Notation

α: order of reaction with respect to 1-heptyne.
β: order of reaction with respect to hydrogen.
A: Arrhenius preexponential factor.
A_A: preexponential factor of the heat of adsorption of 1-heptyne.
A_B: preexponential factor of the heat of adsorption of 1-heptene.
A_{H2}: preexponential factor of the heat of adsorption of hydrogen.
A_1: preexponential factor of the specific reaction rate constant, k_1.
A_3: preexponential factor of the specific reaction rate constant, k_3.
C_A^0: initial concentration of 1-heptyne (mol L^{-1}).
C_A: concentration of 1-heptyne (mol L^{-1}).
C_B: concentration of 1-heptene (mol L^{-1}).
C_C: concentration of n-heptane (mol L^{-1}).
C_{H2}: concentration of hydrogen in the liquid phase (mol L^{-1}).
C_S: concentration of free sites.
E_A: apparent activation energy (KJ mol^{-1}).
E_{H2}: activation energy for the hydrogen adsorption (KJ mol^{-1}).
E_1: activation energy of the reaction of hydrogenation of 1-heptyne to 1-heptene (KJ mol^{-1}).
E_3: activation energy of the reaction of hydrogenation of 1-heptyne to n-heptane (KJ mol^{-1}).
ΔH: reaction heat (KJ mol^{-1})
$|\Delta H_{H2}|$: absolute value of the enthalpy of hydrogen adsorption (KJ mol^{-1}).
$|\Delta H_A|$: absolute value of the enthalpy of adsorption of 1-heptyne (KJ mol^{-1}).
$|\Delta H_B|$: absolute value of the enthalpy of adsorption of 1-heptene (KJ mol^{-1}).
k: specific reaction rate constant.

* Corresponding Author

K: equilibrium constant (equation (6)).
K_A: adsorption constant for 1-heptyne.
K_B: adsorption constant for 1-heptene
K_C: adsorption constant for n-heptane
K_{H2}: adsorption constant for hydrogen
k_A: direct rate specific constant for 1-heptyne adsorption.
k_{H2}: direct rate specific constant for H_2 dissociative adsorption.
k'_{H2}: direct rate specific constant for H_2 non disociative adsorption.
k_1: direct rate specific constant for 1-heptyne to 1-heptene surface hydrogenation reaction.
k_3: direct rate specific constant for 1-heptyne to n-heptane surface hydrogenation reaction.
P_{H2}: partial pressure of hydrogen (bar).
R: ideal gas universal constant (0.082 L.atm.mol^{-1}.K^{-1}).
r_1: rate of step 1 (mol L^{-1}.h^{-1}).
r_3: rate of step 3 (mol L^{-1}.h^{-1}).
r^0_A: 1-heptyne initial hydrogenation rate (mol L^{-1}.h^{-1}).
T: absolute temperature (K)
t: time.

6. References

[1] L'Argentière PC, Cagnola EA, Quiroga ME, Liprandi DA (2002) A palladium tetra-coordinated complex as catalyst in the selective hydrogenation of 1-heptyne. Appl. Catal. A: Gen. 226: 253-263.

[2] Lennon D, Marshall R, Webb G, Jackson S D (2000) The effect of hydrogen concentration on propyne hydrogenation over a carbon supported palladium catalyst studied under continuous flow conditions. Stud. Surf. Sci. Catal. 130: 245-250.

[3] Nishimura S. (2001) Handbook of Heterogeneous Catalytic Hydrogenation for Organic Synthesis. John Wiley & Sons, Inc. Canadá: ISBN 0-47139698-2, pp. 148-169.

[4] Lindlar H, Dubuis R (1966) Palladium catalyst for partial reduction of acetylenes. Org Synth 46: 89–92.

[5] Lederhos CR., L'Argentière PC, Fígoli NS (2005) 1-Heptyne Selective Hydrogenation over Pd Supported Catalyst. Ind. Eng. Chem. Re.s Devel 44: 1752-1756.

[6] Bennett JA, Creamer NJ, Deplanche K, Acaskie LE, Shannon IJ, Wood J (2010) A comparison of Pd/Al_2O_3 and bio-Pd in the hydrogenation of 2-pentyne. J. Chem. Eng. Sc. 65: 282-290.

[7] Sárkány A, Beck A, Horváth A, Révay Zs, Guczi L (2003) Acetylene hydrogenation on sol-derived Pd/SiO_2. Appl. Catal. A: Gen. 253: 283–292.

[8] Anderson JA, Mellor JL, Wells RPK (2009) Pd catalysed hexyne hydrogenation modified by Bi and by Pb. J. Catal. 261: 208-216.

[9] Evangelisti C, Panziera N, D'Alessio A, Bertinetti L, Botavina M, Vitulli G (2010) New monodispersed palladium nanoparticles stabilized poly-(N-vinyl-2-pyrrolidone): Preparation, structural study and catalytic properties. J. Catal. 272: 246-252.

[10] Mastalir A, Király Z (2003) Pd nanoparticles in hydrotalcite: mild and highly selective catalysts for alkyne semihydrogenation. J. Catal. 220: 372–381.

[11] Lederhos CR, Badano JM, Quiroga ME, Coloma-Pascual F, L'Argentière PC. (2010) Influence of Ni addition to a low-loaded palladium catalyst on the selective hydrogenation of 1-heptyne. Quim. Nova 33(4): 816-820.

[12] Lederhos CR, Maccarrone MJ, Badano JM, Coloma-Pascual F, Yori JC, Quiroga ME (2011) Hept-1-yne partial hydrogenation reaction over supported Pd and W catalysts. Appl. Catal. A: Gen. 396: 170-176.

[13] Alves JA, Bressa SP, Martínez OM, Barreto GF (2007) Kinetic study of the liquid-phase hydrogenation of 1-butyne over a commercial palladium/alumina catalyst. Chem. Eng. J. 125 (3): 131-138.

[14] Crespo-Quesada M, Dykeman RR, Laurenczy G, Dyson PJ, Kiwi-Minsker L (2011) Supported nitrogen-modified Pd nanoparticles for the selective hydrogenation of 1-hexyne. J. Catal. 279 (1): 66-74.

[15] Maccarrone MJ, Lederhos C, Badano J, Quiroga ME, Yori J C (2011) Liquid-phase selective hydrogenation of 1-heptyne over Ni/Al_2O_3. Effect of the reaction temperatura. Avances en Ciencias e Ingeniería 2 (2): 59-68.

[16] Boudart M, Hwang HS (1975) Solubility of hydrogen in small particles of palladium J. Catal. 39: 44-52.

[17] Hu S, Chen Y (1998) Partial hydrogenation of benzene: A review. J. Chin. Chem. Eng. 29: 387-396.

[18] L'Argentière P C, Cañón MM, Fígoli NS, Ferrón (1993) AES and XPS Studies of the Influence of Ni Addition on Pd/Al_2O_3 Catalytic Activity and Sulfur Resistance. J. Appl. Surf. Sci. 68: 41-47.

[19] NIST X-ray Photoelectron Spectroscopy Database NIST Standard Reference Database 20. Version 3.5 (Web Version). National Institute of Standards and Technology. USA. (2007)

[20] Telkar MM, Nadgeri JM, Rode CV, Chaudhari RV (2005) Role of a co-metal in bimetallic Ni–Pt catalyst for hydrogenation of m-dinitrobenzene to m-phenylenediamine. Appl. Catal. A: Gen. 295: 23–30.

[21] Juan-Juan J, Roman-Martinez MC, Illan-Gomez MJ (2004) Catalytic activity and characterization of Ni/Al_2O_3 and NiK/Al_2O_3 catalysts for CO_2 methane reforming. Appl. Catal. A: Gen. 264: 169-174.

[22] Web Page: www.lasurface.com/accueil/index.php

[23] Wagner CD, Riggs WM, Davis RD, Moulder JF (1978). In Handbook of X-ray Photoelectron Spectroscopy. Muilenberg. G.E., Ed. Perkin-Elmer: Eden Preirie, MN.

[24] Dantas Ramos AL, da Silva Alves P, Aranda DAG, Schmal M (2004) Characterization of carbon supported palladium catalysts: inference of electronic and particle size effects using reaction probes. App. Catal. A: Gen. 277 (1-2): 71-81.

[25] Benitez VM, Querini CA, Fígoli NS, Comelli RA (1999) Skeletal isomerization of 1-butene on WO_x/γ -Al_2O_3. Appl. Catal. A: Gen. 178: 205-218.

[26] Huang S, Zhang C, He H (2008) Complete oxidation of o-xylene over Pd/Al_2O_3 catalyst at low temperature. Catal Today 139: 15-23.

[27] Salagre P, Fierro JLG, Medina F, Sueiras JE (1996) Characterization of nickel species on several γ -alumina supported nickel samples. J. Molec. Catal. A: Chem. 106 125-134.

[28] Heracleous E, Lee AF, Wilson K, Lemonidou AA (2005) Investigation of Ni-based alumina-supported catalysts for the oxidative dehydrogenation of ethane to ethylene: structural characterization and reactivity studies. J. Catal. 231: 159-171.

[29] Ferrer V, Moronta A, Sánchez J, Solano R, Bernal S, Finol D (2005) Effect of the reduction temperature on the catalytic activity of pd-supported catalysts. Catal. Today 107: 487-492.

[30] Hou Z, Yokota O, Tanaka T, Yashima T (2003) Characterization of Ca-promoted Ni/γ-Al_2O_3 catalyst for CH_4 reforming with CO_2. Appl. Catal. A: Gen 253: 381-387.

[31] Hoffer BW, van Langeveld AD, Janssens JP, Bonne RLC, Lok CM, Moulijn JA (2000) Stability of highly dispersed Ni/Al_2O_3 catalysts: Effects of pretreatment. J. Catal. 192: 432-440.

[32] Li F, Yi X, Fang W (2009) Effect of Organic Nickel Precursor on the Reduction Performance and Hydrogenation Activity of Ni/Al_2O_3 Catalysts. Catal. Let.t 130: 335–340.

[33] Mallat T, Baiker A (2000) Selectivity enhancement in heterogeneous catalysis induced by reaction modifiers. App. Catal. A: Gen. 200: 3-22.

[34] Joback KG. Unified Approach to Physical Property Estimation Using Multivariate Statistical Techniques, M.S. Thesis, MIT, Cambridge, MA, (1984).

[35] Sierra Jimenez F, "Algunos aspectos modernos del fenómeno de la adsorción". 22 (1945) Universidad de Murcia, Servicio de Publicaciones.

[36] Semagina N, Renken A, Kiwi-Minsker L (2007) Monodispersed Pd-nanoparticles on carbon fiber fabrics as structured catalyst for selective hydrogenation. Chem. Eng. Sc. 62 (18-20): 5344-5348.